Semiconductor Traps for Laser-Cooled Atomic Ions and Scalable Quantum Computing

D. Stick[1], W. K. Hensinger[1,2], S. Olmschenk[1], C. Monroe[1]*

Abstract

The electromagnetic confinement of atomic ions has provided a useful testbed for many different applications in atomic physics, including laser cooling {1}, mass spectrometry {2}, and precision control of nearly-pure quantum states {3}. Recently, ion traps have been effectively applied to the growing field of quantum computation {4}, where the ability to isolate a single ion from its environment has made it an attractive architecture for a large-scale quantum information processor {5, 6, 7}. While many of the fundamental quantum computing building blocks have been demonstrated with trapped ions {8}, the technology for scaling to large numbers of ion quantum bits (qubits) is just beginning to develop. In this paper, we describe an important milestone on this path with the successful operation of an ion trap fabricated on an integrated gallium arsenide (GaAs) heterostructure, which could in principal scale to host a large array of ions.

Introduction

Quantum information science incorporates concepts from multiple disciplines, including physics, mathematics, electrical engineering, and computer science. The unifying characteristic that distinguishes it from familiar classical information science is that it takes advantage of the unique quantum mechanical properties of superposition and entanglement to store and manipulate information in a massively parallel manner {4}. The problems for which quantum computers are exceptionally well equipped are currently restricted to a few general and important categories, such as factoring and database searching. As transistors approach the atomic scale in size and Moore's law reaches its end, quantum computers may play an increasing role in the future of computing.

An ion trap holds individual atomic ions using a combination of oscillating RF electric fields and static fields which form a harmonic confining potential{9, 2}. For quantum computing applications, atomic ions are chosen that have only one valence electron, with internal electronic states similar to hydrogen. In the particular case of cadmium ions used in our experiments, the qubit is stored in a pair of hyperfine electronic ground states, which arise from the interaction between the electron magnetic moment with that of the nucleus. Such "spin" states form an ideal qubit for the same reason that they are used for atomic clocks: they are stable, long-lived, and can store coherence for very long times.

Various schemes for implementing logic gates and entangling multiple ions are available, most of which involve coupling the internal state of the ion with its motion via Coulomb repulsion {5, 10, 6}. The motional modes of collective ion motion in a linear trap can be accurately modeled as a quantum harmonic oscillator. By applying lasers that apply a force depending upon the qubit state, multiple ions can be entangled through their collective motion.

The successful implementation of the basic building blocks of a quantum computer does not, however, ensure its large-scale viability. Since any interaction of the qubit state with the environment destroys the quantum information, great care must be taken to isolate the qubit. Because even low error rates cannot be tolerated in a large calculation, quantum error correction algorithms {11, 12, 13} have been devised to store the information redundantly and correct any errors that occur. While this relaxes the level of control required to perform an operation, the

1 FOCUS CENTER AND DEPARTMENT OF PHYSICS, UNIVERSITY OF MICHIGAN,
ANN ARBOR, MICHIGAN 48109, USA
2 DEPARTMENT OF PHYSICS AND ASTRONOMY, UNIVERSITY OF SUSSEX, BRIGHTON, EAST SUSSEX, BN1 9QH,
UNITED KINGDOM
*EMAIL: DSTICK@UMICH.EDU

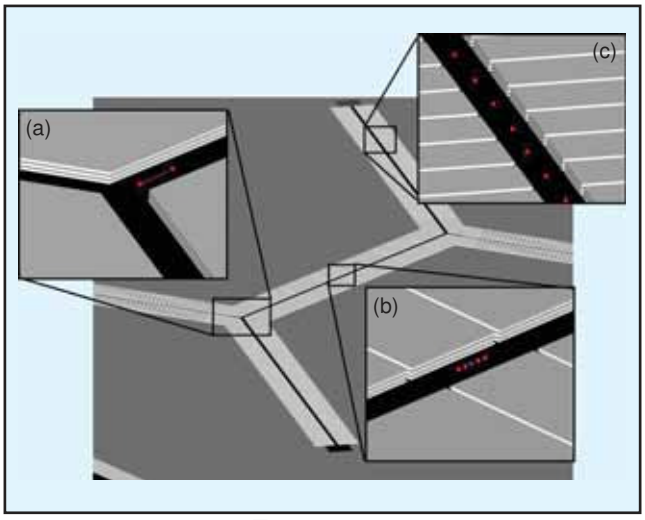

Figure 1: Ion traps array. The insets show regions with specific functions, like a junction through which ions can be shuttled (a), an interaction region (b), and a region for ion storage (c).

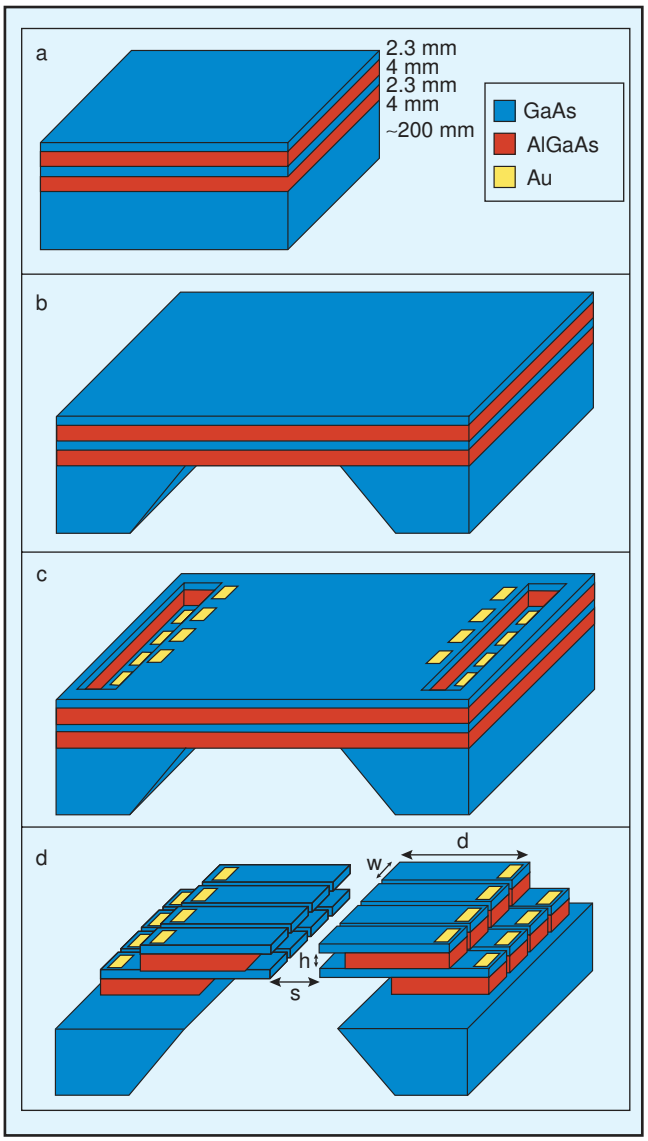

Figure 2: Processing steps. (a) MBE grown GaAs/AlGaAs heterostructure. (b) Backside etch. (c) Bond pads. (d) Cantilever etch.

overhead is not insignificant, particularly in the number of trapped ions required. Depending on the scheme, between 10 and 30 ions are required per qubit, with most of those being error correcting spectator ions. Given this overhead, a few thousand ions would may be necessary for implementing a useful and viable trapped ion quantum computer. This technological hurdle is the motivation for our research into lithographically fabricated ion traps.

Trapping Geometries

Many different trap geometries can be used to reliably capture and store ions. The feature common to all of them is an oscillating RF voltage applied to certain electrodes, creating a time averaged harmonic potential in which the ion is trapped. In the case of a "linear" trap, the trapping potential due to the RF voltage has a nodal minimum along a line and provides transverse confinement. Static voltages applied to "endcap" electrodes are used in order to confine the ions along the nodal axis. A common type of linear trap consists of two or three layers of ceramic substrates with gold electrodes patterned on the surface {14, 15, 16}. This is not a scalable architecture, since the layers are independently machined and aligned, and the traps cannot be easily miniaturized.

One way to meet the scalability requirement is to take advantage of the fabrication techniques developed for the semiconductor and MEMS industries. There are two general approaches to this problem: traps made on a surface {19, 20}, where the RF node lies above the surface, and multilayer traps {21}, such as the two layer trap discussed here, where the RF node lies between the electrodes. While surface traps are relatively easy to fabricate, the trap depth is typically small and laser access is constrained to coming in from the sides, across the surface. Multilayer traps are more difficult to fabricate, but they offer good optical access through the trap (figure 2d) and the depths can generally be larger. Hybrid schemes combining both types of traps have also been proposed.

Both types of traps take advantage of photolithography to precisely create multiple adjacent ion traps, which could be scaled to many traps in a complicated array, as seen in figure 1. In this schematic there are many different trapping zones, some with specialized functions. These include regions for ion storage and interaction, as well as junctions {16} for moving ions arbitrarily in relation to each other. Another advantage of photolithography is its flexibility; scaling from a single trap to a large array would not require a major change in the process, but just a different mask. One downside is that the size of the structure is restricted in the vertical dimension, which reduces the trap strength for a given voltage by up to $1/\pi$ {21}. More importantly, the materials used in semiconductor and MEMS processing are often not suitable for ion traps, which require high voltage RF potentials to be applied. The competing requirements of low capacitance to ground and low RF loss in the conducting materials, as well as high voltage breakdown in the insulators, place limitations particularly on the vertical geometry of these structures.

Fabrication

The traps we report here were fabricated from GaAs/AlGaAs heterostructures which were grown on a GaAs substrate using molecular beam epitaxy (figure 2a). The substrate is heavily

doped with Si (n type), and on top of it is a 4 μm layer of $Al_{.7}Ga_{.3}As$ for electrical insulation, a 2.3 μm layer of doped GaAs (3×10^{18} e/cm^3), another identical insulating AlGaAs layer, and an identical top layer of doped GaAs.

The first processing step is a backside etch that creates a hole over which the trap cantilevers will suspend. This is done in two parts: first a piranha etch (sulfuric acid and hydrogen peroxide) to remove the bulk of the material, followed by a selective etch of citric acid and peroxide, which is much slower but preferentially etches the GaAs, stopping on the bottom AlGaAs layer (figure 2b).

Next, a photolithography step exposes the location of a future electrical contact to the substrate. A dry etch is performed with an Inductively Coupled Plasma (ICP) reactive ion etcher down to this layer. A subsequent photolithography step and ICP etch exposes future contacts to the second, lower GaAs layer. Bond pads with Ni, Ge, and Au are evaporated with an electron beam evaporator to form the contacts which are annealed at a maximum temperature of 450°C (figure 2c). The electrodes are separated from their neighbors with an ICP etch, at which point the structure has taken its recognizable shape. Finally, the whole device is chemically etched in concentrated HF, which selectively etches the insulating AlGaAs back about 15 microns from the edge of the cantilevers (figure 2d). This is done to prevent stray charge from building up on the AlGaAs and affecting the ion. SEM images of a representative GaAs ion trap can be seen in figure 3.

The ion trap chip is then mounted and wirebonded to a ceramic chip carrier. Surface mount capacitors (1000 pF) are used to RF ground each DC electrode. In the particular ion trap we describe here, the substrate ground was not connected.

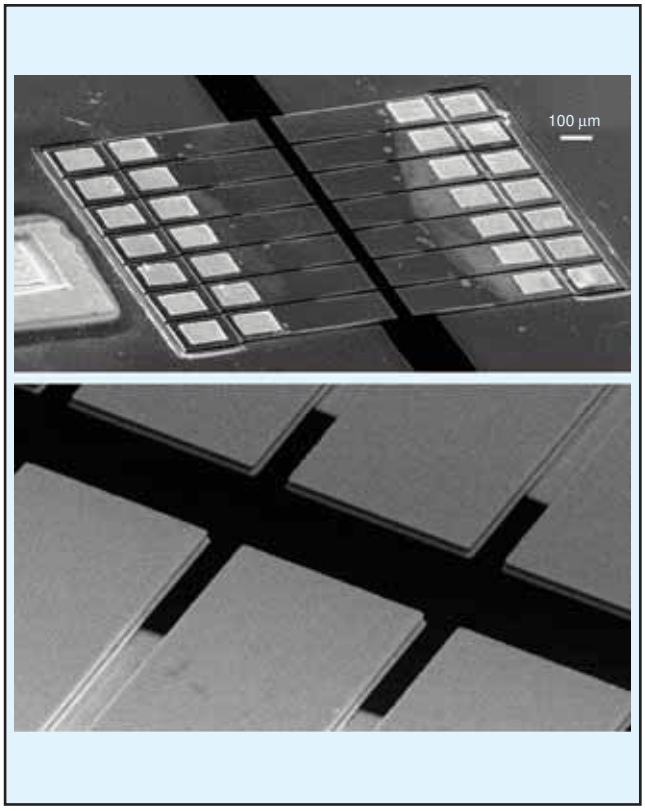

Figure 3: SEM of an ion trap. The top figure shows the cantilevers as well as the bond pads (at the back of the cantilevers) to both the top and bottom GaAs layers. The bottom figure is a zoomed in view of the trapping region.

Operation

We operated the trap with an RF drive frequency of 15.9 MHz and a voltage amplitude of 8 V. We used static potentials of 1.00 V on the outside electrodes and -0.33 V on the inside electrodes. The harmonic potential due to the combination of oscillating and static fields can be characterized with the ion's frequency of oscillation in the trap, called the secular frequency. The GaAs trap had a measured axial secular frequency of $\omega_z/2\pi$=1.0 MHz (see figure 2d), with transverse secular frequencies of $\omega_{x'}/2\pi$=3.3 MHz and $\omega_{y'}/2\pi$=4.3 MHz. The x' and y' vectors are defined by the eigenvectors of the Hessian matrix of the potential function (often referred to as the principal axes); they are rotated ~ 40° from the x and y directions, as found from computer simulations. This is an important characteristic; since the laser going through the trap does not have any component of its k vector in the x direction, it would not Doppler cool the ion if one of its principal axes were also in the x direction. An image of a single trapped cadmium ion is shown in figure 4.

In terms of trap strength, the most significant restriction was the maximum RF voltage we could apply. While we applied up to 70 volts DC between the top and bottom cantilevers, we could only apply 11 volts of RF (14.75 MHz) to a trap before breakdown. The suspected cause is RF power dissipation which heats the cantilevers. In general, for an applied voltage V_0 at a frequency Ω_T, the power dissipated in the trap is $P_D = V_0^2 C \Omega_T / (2Q)$, where C is the total capacitance from the RF electrodes to ground,

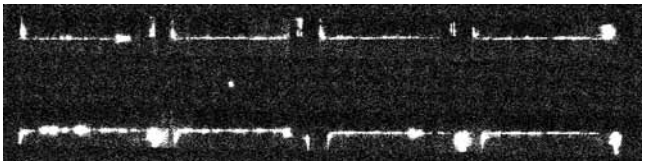

Figure 4: Image of an ion in a trap. This is an overhead view of the trap, where the light is scattering from the edges of the electrodes. An ion appears between the second set of electrodes from the left.

and Q is the quality factor of the trap structure. Q describes the losses in the electrodes, and is given by $1/Q = R_S C \Omega_T + \tan\delta$, where R_S is the net series resistance of the RF electrodes and $\tan\delta$ is the loss tangent of the insulation layer in this experiment, $Q \sim 55$, which is consistent with a direct electrical measurement of 20 Ω for a single cantilever and $C \sim 34$ pF.

Qubits are stored in the ground state hyperfine levels of the ion, denoted by $\uparrow$ (singlet) and $\downarrow$ (triplet) and separated in energy by $\Delta E = h\omega_{HF}$, where $\omega_{HF}/2\pi = 14.53$ GHz. To detect the qubit state, we illuminate the ion with cw radiation near 214.5 nm, produced by frequency-quadrupling the output of a Ti-Sapphire laser. This "detection beam" is resonantly tuned to a transition linking the $\downarrow$ state to an excited electronic state of the ion. When the ion is in the state $\downarrow$, it gets excited and then decays back to the $\downarrow$ state, emitting a photon which can be detected by a photomultiplier tube or CCD camera. If the ion is in the $\uparrow$ state, the beam is very far from resonance and it is not excited.

An important characteristic of an ion trap is the rate at which it heats an ion, since many of the proposed entanglement and gate schemes use the ion's motional modes. It is also because of this heating that we must continuously Doppler cool the ion, using the same laser beam as the detection beam but bringing the applied UV light slightly below resonance with the acousto-optical modulator. In this experiment, the heating rate of the ion was determined by measuring the suppression of the stimulated Raman transition rate between the qubit states after multiple delay times without cooling. The hotter the ion is the slower the Raman transition rate, as characterized by the Debye-Waller factor. The Raman beams are generated in a similar fashion as the above mentioned detection beam. The Raman transition rate is measured by performing the following sequence {22}: 1) Optically pumping the ion to the $\uparrow$ quantum state. A beam resonant between the $\downarrow$ and excited state is applied. If the electron decays to the $\uparrow$ state it remains there, and otherwise gets excited again and decays until it falls into the $\uparrow$ state. 2) A stimulated Raman transition is driven by applying light tuned ~ 70 GHz below an excited P state. A resonant electro-optical modulator is placed in front of the second doubling cavity with a frequency of $(\omega_{HF}/2\pi)/2$. The cavity is adjusted to have a free spectral range of $(\omega_{HF}/2\pi)/4$ so that all EOM sidebands build up in the cavity. By applying a phase shift with a Mach-Zehnder interferometer to prevent the net Raman transition from disappearing due to destructive interference, Rabi flopping can be driven between each pair of spectral components separated by ω_{HF}. 3) Measure the qubit state, as described above.

Our measured heating rate, ~1 quanta per μs, was significantly higher than that of other traps. Supporting this was the observation that the ion would "boil" out of the trap after ~100 ms without Doppler cooling, versus times of hours in other traps. Additionally, the lifetime of the ion in the trap while being Doppler cooled was about ten minutes, versus hours or days for other traps. A higher heating rate than larger traps was expected, due to the small size of the trap and the strong dependence of heating on the ion-electode distance {23}. However, trap size alone could not account for the measured high heating rate, so we suspect some mechanism of heating other than fluctuating regions of voltage noise on the electrodes (patch potentials) {24}. A proposed mechanism is the piezoelectric effect in GaAs {25}, through which electrically driven mechanical oscillations could heat the ion. Another possibility is that there is a mechanical resonance of the ion trap which overlaps with the secular frequency, though given the calculated Q on the order of 1000, this seems unlikely. Future experiments will seek to determine and decrease this anomalous heating.

Conclusion

The GaAs trap described here was a first step in the direction of learning what parameters and constraints are important in constructing and operating a semiconductor fabricated microtrap. These include minimizing the capacitance of each trap, shrinking the electrode size, and minimizing heating of the ion, to name a few. Given the success of this demonstration, we intend to fabricate different structures which may show lower heating rates and have higher trap depths. We also plan to fabricate crossing junctions, which would allow multiple ions to be shuttled arbitrarily in relation to each other, a necessary capability for some ion trapped quantum computing schemes. The fabrication techniques developed would also be potentially useful for building a three layer structure, and with some adaptations, constructing the trap out of other materials like silicon. With the work described here and the ongoing efforts of other ion trapping groups, we anticipate great strides in solving the problem of constructing large scale ion trap arrays for quantum computation.

Acknowledgments

We acknowledge useful discussions with J. A. Rabchuk, S. Horst, T. Olver, K. Eng, P. Lee, P. Haljan, K.-A. Brickman, L. Deslauriers and M. Acton. We particularly thank Keith Schwab and the Laboratory for Physical Sciences for providing expertise and facilities to make this research possible. This work was supported by the US Advanced Research and Development Activity and National Security Agency under Army Research Office contract W911NF-04-1-0234, and the National Science Foundation Information Technology Research Program.

References

{1} Metcalf, H.J. & van der Straten, P. Laser Cooling and Trapping (Springer, NY, 1999).

{2} Paul, W. Electromagnetic traps for charged and neutral particles, Rev. Mod. Phys 62, 531,(1990).

{3} Leibfried, D., Blatt, R., Monroe, C. & Wineland, D.J. Quantum dynamics of single trapped ions. Rev. Mod. Phys 75, 281-324 (2003).

{4} Nielsen, M.A. & Chuang, I. L. Quantum Computation and Quantum Information (Cambridge Univ. Press, Cambridge, 2000).

{5} Cirac, J.I. & Zoller, P. Quantum computations with cold trapped ions. Phys. Rev. Lett. 74, 4091-4094 (1995).
{6} Cirac, J.I. & Zoller, P. A scalable quantum computer with ions in an array of microtraps. Nature 404, 579-581 (2000).
{7} Kielpinski, D., Monroe, C. & Wineland, D. J. Architecture for a large scale ion-trap quantum computer. Nature 417, 709-711 (2002).
{8} Schmidt-Kaler, F., et al,. Nature 422, 408 (2003); Chiaverini, J. et al., Science 308, 997 (2005); Brickman, K.A. et al., Phys. Rev. A 72, 050306(R) (2005).
{9} Dehmelt, H.G. Radiofrequency spectroscopy of stored ions I: Storage. Adv. At. Mol. Phys 3, 53-73 (1967).
{10} Molmer, K., & Sorensen, A. Phys. Rev. Lett. 82}, 1835 (1999); Milburn, G.J., Schneider, S., & James, D.F.V. Fortschr. Physik 48, 801 (2000).
{11} Shor, P.W. Scheme for reducing decoherence in quantum computer memory. Phys. Rev. A 52, R2493 (1995).
{12} Steane, A. Efficient fault tolerant quantum computing. Nature 399, 124-126 (1999).
{13} Chiaverini, J., et al., Realization of quantum error correction. Nature 432, 602-605 (2004).
{14} Rowe, M.A., et al., Transport of quantum states and separation of ions in a dual rf ion trap. Quantum Inf. Comput 2, 257-271 (2002).
{15} Deslauriers, L., et al., Zero-point cooling and low heating of trapped Cd ions. Phys. Rev. A 70, 043408 (2004).
{16} W. K. Hensinger, et al., T-junction ion trap array for two-dimensional ion shuttling, storage, and manipulation. Appl. Phys. Lett. 88, 034101 (2006).
{17} Turchette, Q.A., et al., Heating of trapped ions from the quantum ground state. Phys Rev. A 61, 063418 (2000).
{18} Blinov, B., et al., Sympathetic cooling of trapped Cd isotopes. Phys. Rev. A 65, 040304 (2002).
{19} Chiaverini, J., et al., Surface electrode architecture for ion-trap quantum information processing. Quantum Inf. Comput 5, 419-439 (2005).
{20} Seidelin, S., et al., A microfabricated surface-electrode ion trap for scalable quantum information processing. preprint at <http://arxiv.org/abs/quant-ph/0601173>.
{21} Madsen, M.J., et al., Planar ion trap geometry for microfabrication. Appl. Phys. B 78, 639-651 (2004).
{22} Lee, P.J., et al., Atomic qubit manipulations with an electro-optic modulator. Optics Letters 28, 1582-1584 (2003).
{23} Deslauriers, L., et al., Scaling and suppression of anomalous heating in ion traps. preprint: http://arxiv.org/abs/quant-ph/0602003.
{24} Camp, J.B., Darling, T.W., & Brown, R.E. Macroscopic variations of surface potentials of conductors. J. Appl. Phys. 69, 7126 (1991).
{25} Private communications with G. Milburn.